한국측지학회지, 제 13 권, 제 2 호, pp.299~307(1995년 12월 30일)

Distinct Point Detection : Förstner Interest Operator

Cho, Woo-Sug*

ABSTRACT

The extraction of distinct points such as corner points and circular features is a basic procedure in digital photogrammetry and computer vision. This paper describes the extraction of image features from the raw images (gray value images), especially Förstner interest corner points. The mathematical model of the Förstner interest operator as well as the behavior in the presence of noise are investigated. Experiments with real images prove the feasibility of the Förstner interest operator in the field of Digital Photogrammetry.

要　　旨

본 논문은 수치영상으로부터 Digital Photogrammetry와 Computer Vision 분야에서 위치결정 및 3차원 정보의 자동추출을 위한 기본단계인 Distinct Point 추출기법중 Förstner interest operator에 관한 연구이다. Gradient에 기초한 Förstner interest operator는 Orientation-invariant의 특징을 가지고 있으며 소정의 Subpixel 정확도를 얻을 수 있다.

본 연구에서는 Föstner interest operator에서 얻어진 Corner Points와 Circular Features를 구분하기 위한 방법으로 F-test를 적용하였으며 Nosie가 Förstner interest operator에 미치는 영향을 고찰하였고 실제 사진영상에 Förstner interest operator를 도입하여 실효성에 바탕을 둔 적용 여부를 검증하였다.

1. Introduction

With digital imagery from various sources as well as high performance computer hardware and software, the automation in photogrammetric processes such as relative orientation, aerial triangulation, and surface reconstruction becomes possible. One of most fundamental tasks in photogrammetry is to find conjugate features in two or more images, which is commonly referred to as the matching problem.

Medioni and Nevatia [1984] argue "the higher the level of descriptions at which mathching is attempted, the more likely the desciptions are to be invariant to imaging changes, but this gain may be offset by the errors and deficiencies of the current programs that compute these descriptions". It is true that the invariance of high level descriptions facilitates the matching process, but a good high level desciption can only be extracted after the image has been interpreted [Vosselman 1992]. Considering a comprise between invariance and correctness of feature descriptions, point feature extraction is a primary concern in most automatic photogrammetric procedures.

There has been much research in the field of distinct point detection [Moravec 1977, Dreschler and Nagel 1981, Mikhail 1984, Förstner and Gülch 1987, Förstner 1994, Tang and Heipk 1994]. These previous works show that the Moravec operator and the Fürstner interest operator perform best for real images. Compared with the Moravec operator, the Förstner interest operator has the salient features such as rotation invariant and subpixel accuracy.

2. Förstner Interest Operator

The implementation of the interest operator con-

*The Ohio State University

sists mainly of three steps:

1. Selection of optimal windows for point detection.
2. Classification of selected windows.
3. Determination of the point location within the selected optimal windows.

The mathematical model of the interest operator is first discussed before the fine details of the above three main steps.

2.1 Mathematical Model

It is assumed that an $n \times n$ window contains a distinct point $g_o=(r_o,c_o)^T$ and the edgel(edge element) at each pixel within the window is defined as a straight line passing through $g_i=(r_i, c_i)^T$ with an orinetation derived from its gradient ∇g_i (see Figure 1(a)). The gradient $\nabla g_i=(g_{ri}, g_{ci})=(\partial g_i/\partial r_i, \partial g_i/\partial c_i)$ can be estimated by any available gradient operator such as the Robert gradient operator.

A conrner point can be estimated from the intersection of all edgels, which is the point closest to all straight lines. The straight line passing through $g_i=(r_i, c_i)^T$ parallel to the edge direction is given by the following equation

$$(g-g_i)^T f_i = 0 \qquad (2.1)$$

where $f_i = \nabla g_i^T = (g_{ri}, g_{ci})^T = |\nabla g_i| \cdot (\cos\phi_i, \sin\phi)^T$

Assuming that each edgel is independent and uncertainty is included in $g_i^T \cdot f_i$, the above equation reads as

$$l_i = \cos\phi_i \cdot r_o + \sin\phi_i \cdot c_o + n_i, \; i = 1, \ldots, n\times n(=m) \qquad (2.2)$$

where $l_i=l(r_i,c_i)=\cos\phi_i \cdot c_i + \sin\phi_i \cdot c_i$ and $n_i=(r_i, c_i)$. It is assumed that the weight of each straight line is proportional to the absolute gradient squared

$$w_i = g_{ri}^2 + g_{ci}^2 \qquad (2.3)$$

This assumption is based on the fact that the precision of point location is dependent on the strength

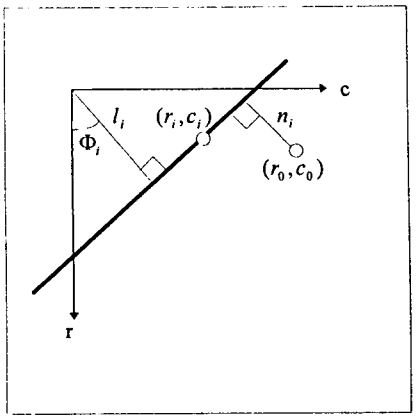

(a)

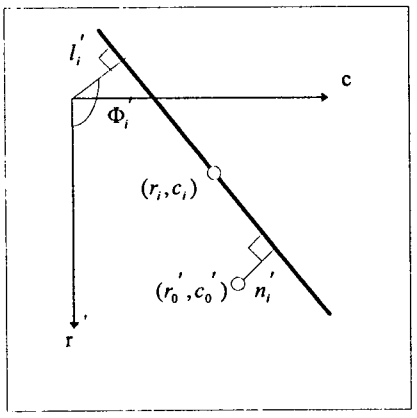

(b)

Fig. 1. Edge element model (a) and Slpoe element model (b) for the Frstner interest operator.

of the gradient. Minimizing $\Omega(r_o, c_o) = \sum_{i=1}^{m} n_i^2 \cdot w_i$ with respect to $\hat{r_o}$ and $\hat{c_o}$ leads to the following normal equation system

$$\begin{bmatrix} \sum g_r^2 & \sum g_r g_c \\ \sum g_r g_c & \sum g_c^2 \end{bmatrix} \begin{bmatrix} \hat{r_o} \\ \hat{c_o} \end{bmatrix} = \begin{bmatrix} \sum g_r^2 \cdot r + \sum g_{g_c} \cdot c \\ \sum g_r g_c + \sum g_c^2 \cdot c \end{bmatrix} \qquad (2.4)$$

A circular feature such as a blob or ring can be also estimated using slope elements (slopels). For corner point estimation, straight lines passing through the points parallel to the edge direction are used for corner point estimation (see Figure 1(b)).

For circular features, straight lines going through the points orthogonal to the edge direction are considered. These straight lines intersect at the center of the circular feature. The equation for the straight lines is

$$(g-g_i)^T f'_i = 0 \tag{2.5}$$

where $f'_i = \nabla g_i^T = |\nabla g_i| \cdot (-\sin\phi, \cos\phi)^T$ The corresponding linear equation (2.6) and target function (2.7) are

$$l_i = -\sin\phi_i \cdot r'_o + \cos\phi_i \cdot c'_o + n'_i, i = 1, \ldots, n\times n(=m) \tag{2.6}$$

$$\Omega'(r'_o, c'_o) = \sum_{i=1}^{m} (n'_i)^2 \cdot w_i \tag{2.7}$$

Using the same weight and minimizing Ω' yields the following normal equation system

$$\begin{bmatrix} \sum g_c^2 & -\sum g_r g_c \\ -\sum g_r g_c & \sum g_r^2 \end{bmatrix} \begin{bmatrix} \hat{r}_o' \\ \hat{c}_o' \end{bmatrix} = \begin{bmatrix} \sum g_c^2 \cdot r - \sum g_r g_c \cdot c \\ -\sum g_r g_c + \sum g_r^2 \cdot c \end{bmatrix} \tag{2.8}$$

The precision of estimated comer point and circular features can be obtained by the following equations, respectively.

$$\hat{D}(\hat{r}_o, \hat{c}_o) = \hat{\sigma}_n^2 \begin{bmatrix} \sum g_r^2 & \sum g_r g_c \\ \sum g_r g_c & \sum g_c^2 \end{bmatrix}^{-1} \tag{2.9}$$

$$\hat{D}(\hat{r}_o', \hat{c}_o') = \hat{\sigma}_n'^2 \begin{bmatrix} \sum g_c^2 & -\sum g_r g_c \\ -\sum g_r g_c & \sum g_r^2 \end{bmatrix}^{-1} \tag{2.10}$$

where $\hat{\sigma}_n^2 = \frac{\Omega(r_o, c_o)}{m-2}$ and $\hat{\sigma}_n'^2 = \frac{\Omega(r_o', c_o')}{m-2}$

2.2 Optimal Window selection

Equations (2.9) and (2.10) show that the precision of estimated point location depends on noise and the signal content of the window, that is, the average squared gradient N. Assuming that noise is constant, the decisive information is only contained in the normal equation matrix N. Thus, the task of selecting an optimal window is reduced to a search for the local optima of the expected precision for the point location.

The search for an optimal window utilizes the following two parameters.

- The size of the error ellipse (w): the average precision of the point or the weight of the point is defined as

$$w = \frac{1}{trN^{-1}} = \frac{detN}{trN} \tag{2.11}$$

- The form of error ellipse (q): the roundness of the error ellipse can be measured by the following equation, which ranges between 0 and 1

$$q = 1 - \left(\frac{\lambda_1 - \lambda_2}{\lambda_1 + \lambda_2}\right)^2 = \frac{4detN}{tr^2N} \tag{2.12}$$

where λ_1 and λ_2 are eigenvalues for the normal equation matrices in (2.4) and (2.8).

From equations (2.11) and (2.12) the two parameters w and q can be directly detdermined from the normal equation matrix N. When q is equal to 1, the error ellipse is circular. When q is equal to 0, the normal matrix is singular, which means that the window does not contain a corner or circular feature but an edge feature. Thus, the q parameter can be used to exclude the points lying on the edges and also can be used to detect the edge points [Förstner 1986].

The selection of an optimal window is based on the following two criteria:

- The error ellipse should be small.
- The error ellipse should be close to a circle.

The first criterion guarantees that the selected optimal window is distinct and separable from its neighborhood and that the accuracy of the es-

timated point location is good. This leads to the following condition

$$w_i \geq w_n, \text{ for all} \in \{\text{neighborhood of i}\}. \quad (2.13)$$

A threshold for weight w_n should be determined with respect to the global image content. There are two ways of selecting the global threshold for weight using the mean or median of weights of all windows in the image. In case of the mean of weights, the threshold for weight is computed as $w_n=f.w_{mean}$ where f is in the range of 0.5 and 1.5. For the median of weght, the threshold for weight is detdermined by $w_n=c \cdot w_{mean}$ Where c ranges from 3 to 5. The two constants f and c had been derived from the previous experiments [Förstner and Gülch 1987].

The circular error ellipse (roundness of error ellipse) ensures that the selected optimal window does not contain strong edge points and strongly oriented texture, but that the point determination is equally precise in all directions. The roundness parameter q should satisfy the condition:

$$q_i \geq q_{min}. \quad (2.14)$$

The threshold for roundness parameter q_{min} can be determined by equation (2.12) using the eigenvalues of the normal equation matrix. The threshold of roundness parameter determines the angle of an interest corner point subtended by two or more linear features. For example, when q_{min} is equal to 0.75, the corresponding ratio between two semiaxes of the error ellipse is $2\sqrt{3}$ and the the corresponding angle is approximately 80°. Previous experiments [Förstner and Gülch 1987] show that the ranger between 0.65 and 0.75 performs well to obtain optimal windows with corner and circular feature points.

2.3 Optimal Window Classification

The optimal window classification decides whether the slected window contains a corner point or a circular feature. Since the edge element model and slope element model are orthogonal to each other, the ratio $\Omega/\Omega'$is Fisher distributed. The test statistic is as follows:

$$T = \frac{\Omega}{\Omega'} \sim F_{m-2,m-2} \quad (2.15)$$

where Ω and Ω' are the weighted sum of squared residuals for edge and slope element models respectively, and m-2 is degree of freedom where m is the number of edge and slope elements of optimal windows. Considering all the optimal windows that contain the edge points are excluded, a two-sided test can be applied as follows:

1. If $T<F_{m-2, m-2, \alpha}$; then corner points.
2. If $T>F_{m-2, m-2, 1-\alpha}$; then circular feature point.

2.4. Optimal point Determination

The optimal point determination aims at eliminating relative local maxima. After optimal window selection and optimal window classification, in many cases the selected windows are close to one another. Using a prespecified window size, each selected optimal window is compared with its neighboring selected windows in term of weights w (2.11). If the weights of its neighboring selected windows are larger than its own weight, the selected window of interest is eliminated from the set of optimal windows. This operation is called non-maxima suppression. The typical window sizes for non-maxima suppression are 5×5 and 7×7.

The location of interest corner point with sub-pixel accuracy is determined by solving the equation (2.4) with the optimal windows after non-maxima suppression. Figure 2 with synthetic test patterns shows examples of corner points at a 99% confidence level. All corner points are detected and well located except the one in the top corner of the triangle in Figure 2(e). Since the q_{min} is set to 0.75, the operator does not select the corner be-

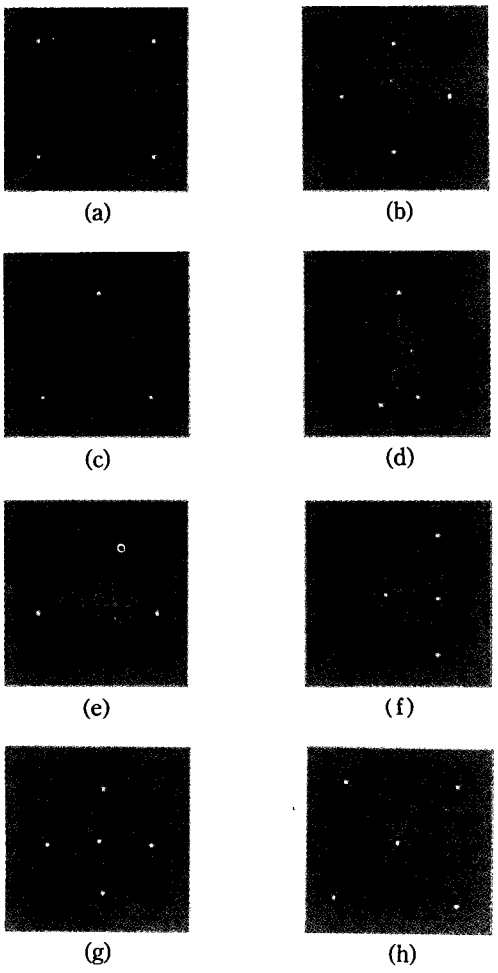

Fig. 2. Interst corner points with 99% confidence using 7×7 window for operator size, 5×5 window for non-maxima suppression, 0.75 for q, and q.5 for f in $W_n = f \cdot W_{mean}$.

cause two edges meet at an angle less than the threshold angle.

As shown in Figure 2, the Förstner interest operator performs well in locating the corner points especially at the area where the intensity of gray values changes abruptly because the edge element and slope element model interact well with those areas. However, when the gradient distribution within the window is not symmetric around the feature, the location of the feature points is shifted. Figure 3 illustrates the case.

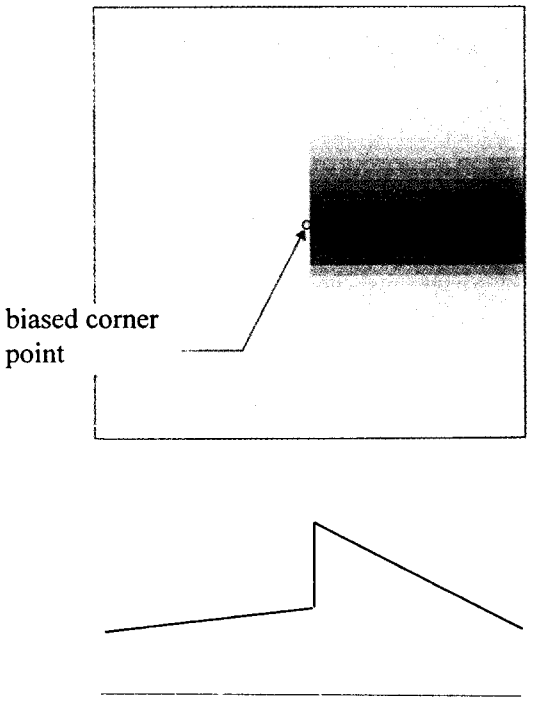

Fig. 3. The bias introduced by interest operator to a step edge where intensity slope is different.

The test image size is 40×40 pixels and the corner point is precisely in center. The intensity slopes at either side of an ideal step edge are different in both row and column directions. This asymmetrical distribution causes a shift; the location of the corner point is at (19.95, 19.35). Heikkilä provided the formula to compute the amount of bias introduced if the slope of the intensity surface at either side of an ideal step edge is different.

The performance of the Förstner interest operator is also influenced by the gradient operator which computes the gradients in an image in the first place. Since the interest operator is rotation invariant, the gradient operator should have the same property.

2.5. Behavior in the Presence of Noise

As demonstrated in the previous section, the Förstner interest operator is sensitive to asymmetrical gradient distributions around features.

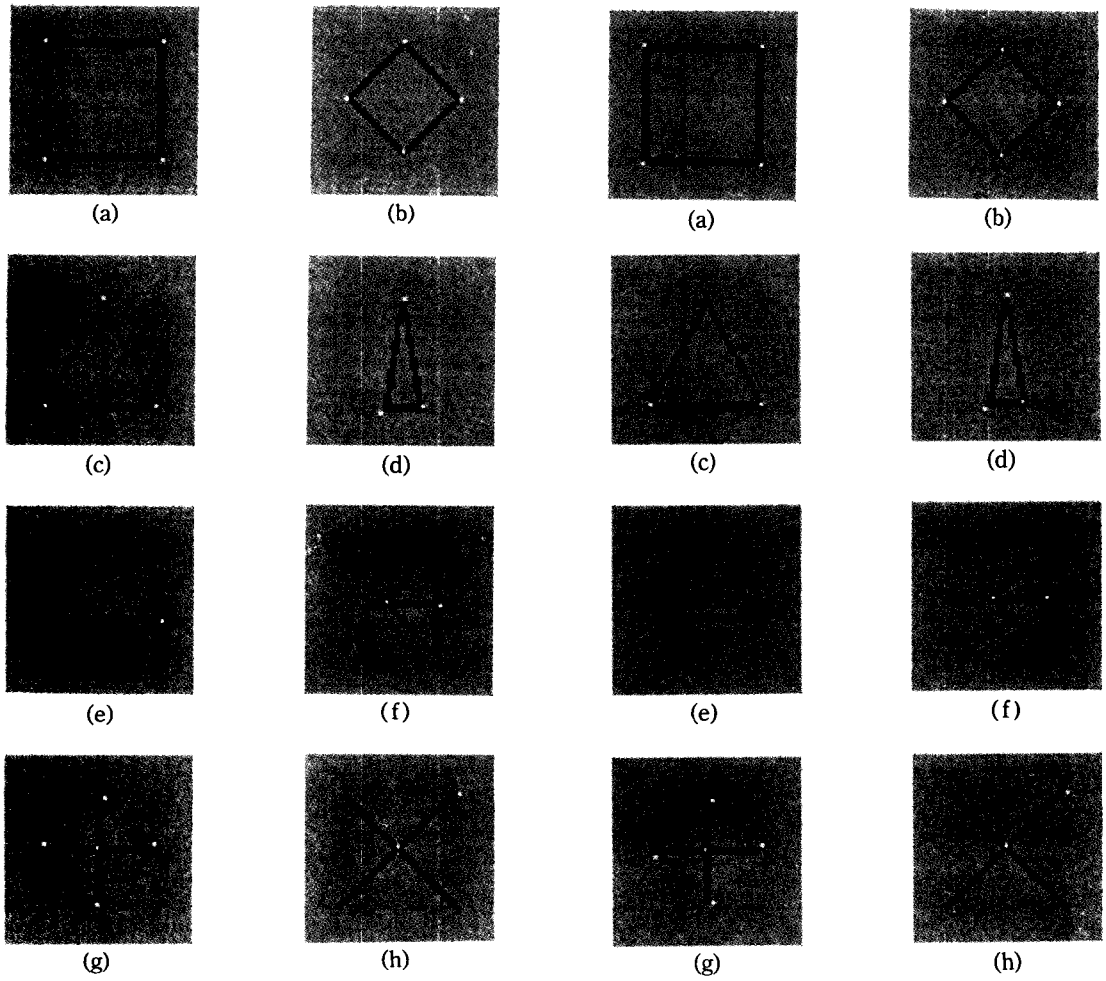

Fig. 4. Interest comer point in synthetic test images with random noise σ = 5.

Fig. 5. Interest corner points in synthetic test with random noise σ = 10.

Here, its sensitivity to noise is examined.

Figure 4, 5, and 6 show eight synthetic images containing random noise of varying degree. The random noise levels (σ=5, 10, and 20) are introduced into the features and background separately. For the Förstner interest operator, the 7×7 window for operator size, 5×5 window for non-maxima suppression, 99% confidence, 0.75 gor q_{min}, and 1.5 for in w_n=f.w_{mean} are used for three different levels of noisy images.

As shown in Figures 4 through 6, the operator fails to detect some corner points which are detected in noise free images (see Figure 2). Moreover, erroneous locations of corner points in images with large random noises are produced. However, the corner points made by two or more edges meeting at right angles are always detected and located mostly within a pixel of the true position even though the random noise σ is equal to 20. Up to noise level σ=10, the interest operator is not much influenced by noise with the exception of some missing corner points corresponding to acute angles.

Since the Förstner interest operator is a gradient based operator, large random noise which generates considerable disturbances of gradient dis-

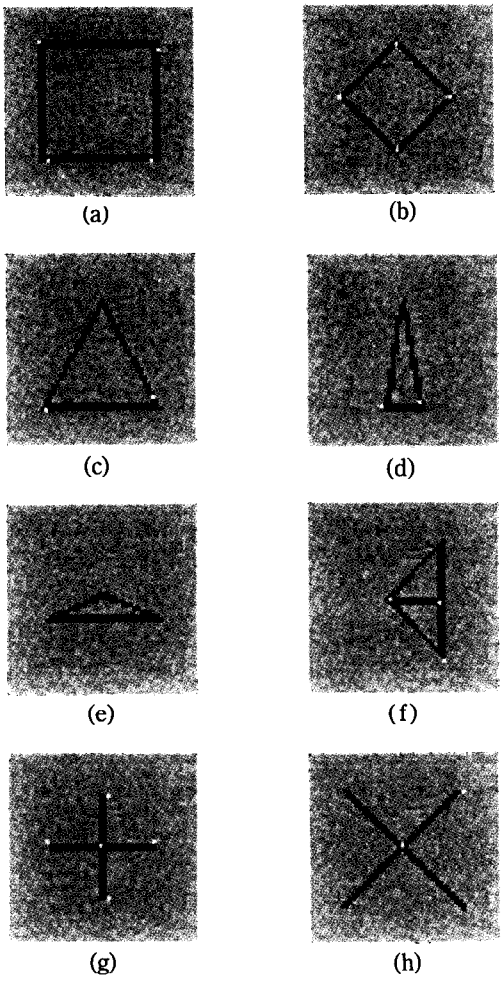

Fig. 6. Interest comer points in synthetic test images with random noise σ = 20

tribution around features deteriorates the performance of the interest operator. Under the noise, the interest operator performs less accurately with 99% confidence especially at corner points with an acute angle. This investigation shows that the Förstner interest operator performs reliably and robustly in noisy images.

3. Experiments and Results

Two images were used in this experiment. The first image depicts the campus of The Ohio State University at a scale of 1:4000. The diapositive was scanned by the Intergraph Photoscan with a

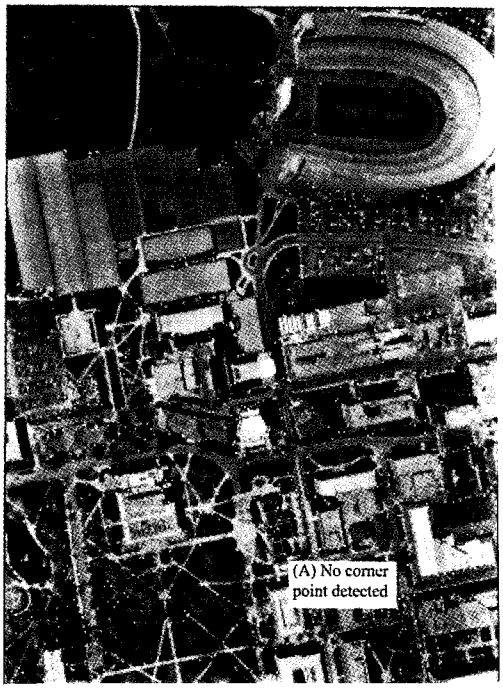

Fig. 7. OSU image superimposed with interest corner points with 99% confidence using 7×7 operator window size 7×7 non-maxima window size, q=0.75, and f=1.5.

resolution of 30μm. An image pyramid was generated using a Gaussian kernel. An image with a resolution 512×512 pixels was used to extract interest corner points. Figure 7 show the image superimposed with corner points.

The second image is from the OEEPE test area Forssa in Southern Finland. The scale is also approximately 1:4000. The image has been scanned with a pixel size of 15 μm using a Zeiss PS1 scanner (see Figure 8). From the image pyramid constructed by using the Gaussian function, the lowest resolution (500×500) image was utilized for the experment.

For corner point detection, the Förstner interest operator requires two thresholds to be set: threshold for weight (f) and threshold for roundness measure (q). In this research, f=1.5 and q=0.75 were used. The corner points were detected at the 97% confidence level. A window size of 7×7 pix-

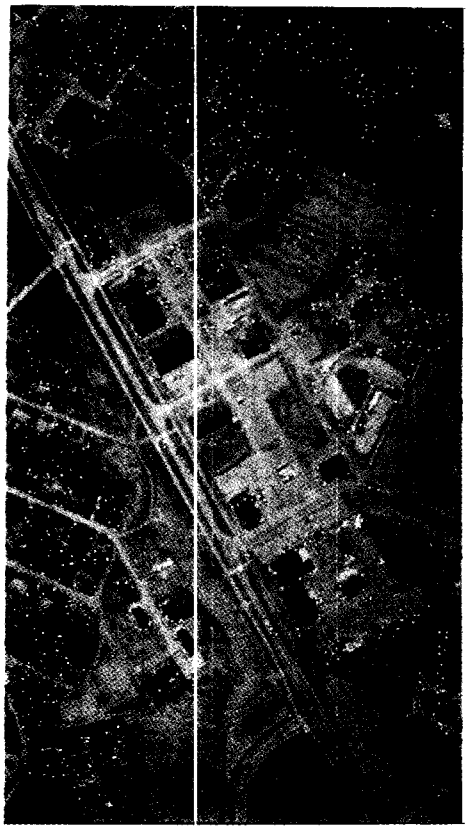

Fig. 8. Forssa image superimposed with interst corner points with 99% confidence using 7×7 operator window size 7×7 non-maxima window size, q=0.75, and f=1.5.

els was used, also for nonmaxima suppression.

The 2×2 Robert gradient operator was employed to compute the gradient. It is important to use an orientation-invariant gradient operator, because the Förstner interest operator is also orientation-invariant. Several gradient operators were tested and was found that the 2×2 Robert operator performs best with the Förstner interest operator.

Table 1. The number of coner points detected by the interest operator

	Number of Detected Corner Points
OSU	1413
Forssa	771

The detected interest corner points after nonmaxima suppression are shown in Figure 7 and 8 by white dots. Most corner points are detected well by the interest operator. However, a closer examination of the OSU campus image reveals that some corner points remained undetected (labeled A in Figure 7). Figure 9 shows the area of point A enlarged together with the corresponding gradients. Point A was not detected because the gradient distribution around the point is not symmetrical--a requirement to pass the threshold criteria for the roundness and strength (parameters q and w). For the two images (OSU and Forssa), the number of corner points detected by the Förstner interest operator is listed in Table 1. As shown in Table 1, the Förstner interest operator detects the corner points enough for further process such as image

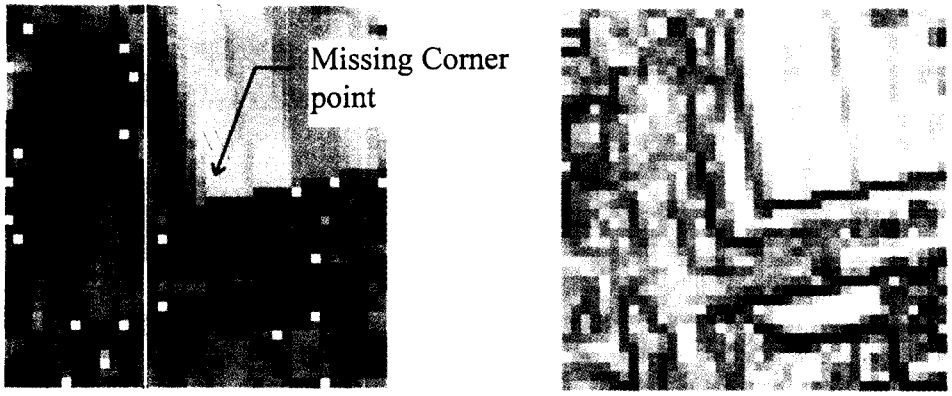

Fig. 9. Image patch and corresponding gradient image containing an undetected corner points caused by gradient disturbance.

matching problem.

4. Conclusion

This paper descibes the detailed desciption of the Förstner interest operator and its implementation with real images. As shown, the Förstner interest operator interacts well with physical features and locates the corner points with subpixel accuracy. However, it was found that the Förstner interest operator performs poorly when the gradient distribution around the features is not symmetrical. This problem can be diminished by convolving the orginal image with smoothing function such as Gaussian function.

Next paper will present the scale space property of the Förstner interest operator and the combination of point feature and linear feature extraction for a high level feature desciption.

References

1. Ballard, Dana H. and Brown, Christopher M. (1982) Computer Vision. Prentice-Hall, Inc.
2. Doorn, B., Agouris, P., Al-Tahir, R., Stefanidies, A. and Zilberstein, O. (1990) Digital Stereo Matching: In perspective. Technical Notes in Photogrammetry No. 10, Department of Geodetic Science and Surveying, The Ohio State University, Columbus, Ohio.
3. Dreschler, L. and Nagel, H. (1981) Volumetric Model and 3D-Trajectory of a Moving Car Derived from Monocular TV-Frame Sequences of a Street Scene. Proceedings of the International Joint Conference on Aritificial Intelligence, Vancouver B.C., 692-697.
4. Ebner, H., and Heipke, C. (1988) Integration of digital image matching and object surface reconstruction. International Archives of Photogrammetry and Remote Sensing, Kyoto, Vol. 27, Part B2, 534-545.
5. Faugeras, O. and Berthod, M. (1980) Scene Labeling; An Optimization Approach. Pattern Recognition, Vol. 12, 339-347.
6. Förstner, Wolfgang (1986) A Feature Based Correspondence Algorithm for Image Matching. International Archive of Photogrammetry Vol. 26-III, Rovaniemi, 1-16.
7. Förstner, Wolfgang and G lch, E. (1987) A Fast Operator for Detection and Precise Location of Distinct Points, Corners and Centers of Circular Features. ISPRS Intercommissiom Workshop, Interlaken, June, 281-305.
8. Förstner, Wolfgang (1994) A Framework for Low Level Feature Extraction. Lecture Notes in Computer Science, Vol. 801, Computer Vision-ECCV'94, 383-394.
9. Heikkilä Jan(1989) Multiscale Representation with F÷rstner Operator. The Photogrammetric Journal of Finland, Vol. 11, No. 2, 40-59.
10. Medioni, Gerad and Nevatia, Ramakant (1984) Matching Images Usign Linear Features. IEEE Transactions on Pattern Analysis and Maching Intelligence, Vol. 6, No. 6, November, 675-685.
11. Mikhail, E.M. and Mitchell, O.R,(1984) Detection and sub-pixel location of photogrammetric targets in digital images, Photogrammetria, 39.
12. Moravec, H.P.(1977) Toward Automatic Visual Obstacle Avidance, Proceedings of the 5th Joint Conference on Artificial Intelligence, Cambridge, 584.
13. Nevatia, R. and Babu, K. R. (1980) Linear Feature Extraction and Description. Computer Graphics and Image Processing, Vol. 13, 257-269.
14. Tang, L. and Heipke, C. (1994) An Automatic Procedure for the Relative Orientation of Aerial Images. Proceedings on Interation, Automation, and Intelligence in Photogrammetry, Remote Sensing and GIS. 3rd Liesmars Colloquium, Wuhan, October, 49-58.
15. Vosselman, George(1994) On the Use of Tree Search Methods in Digitatal Photogrammetry, '94 Munich, ISPRS, Commission III, Delft University of Techology, Delft, The Netherlands.